CHINA PARTICUOLOGY Vol. 2, No. 1, 1–12, 2004

FLOW STRUCTURE FORMATION AND EVOLUTION IN CIRCULATING GAS-FLUIDIZED BEDS

Jie Li[1,2,*] and J. A. M. Kuipers[1]

[1]*Department of Chemical Engineering, Twente University, Enschede, 7500 AE, The Netherlands*
[2]*Materials Science Division, Argonne National Laboratory, Argonne, IL. 60439, USA*
**Author to whom correspondence should be addressed. E-mail: jieli@anl.gov.*

Abstract The occurrence of heterogeneous flow structures in gas-particle flows seriously affects the gas-solid contacting and transport processes in high-velocity gas-fluidized beds. Particles do not disperse uniformly in the flow but pass through the bed in a swarm of clusters. The so-called "core-annulus" structure in the radial direction and "S" shaped axial distribution of solids concentration characterize the typical flow structure in the system.

A computational study, using the discrete particle approach based on molecular dynamics techniques, has been carried out to explore the mechanisms underlying formation of the clusters and the core-annulus structure. Based on energy budget analysis including work done by the drag force, kinetic energy, rotational energy, potential energy, and energy dissipation due to particle-particle and particle-wall collisions, the role of gas-solid interaction and inelastic collisions between the particles are elucidated.

It is concluded that the competition between gas-solid interaction and particle-particle interaction determines the pattern formation in high-velocity gas-solid flows: if the gas-solid interaction (under elevated pressure) dominates, most of particle energy obtained by drag from the gas phase is partitioned such that particle potential energy is raised, leading to a uniform flow structure. Otherwise, a heterogeneous pattern exists, which could be induced by both particle-particle collisions and gas-solid interaction. Although both factors could cause the flow instability, the non-linear drag force is demonstrated to be the necessary condition to trigger heterogeneous flow structure formation. As gas velocity increases and goes beyond a critical value, the fluid-particle interaction suppresses particle collisional dissipation, and as a consequence a more homogeneous flow regime is formed.

Keywords flow structures, particle collision, gas-solid interaction, nonlinear drag, circulating gas-fluidized beds

1. Introduction

The occurrence of heterogeneous flow structures in gas-particle flows seriously affects the quality of gas-solid contacting and transport processes in high-velocity gas-fluidized beds. Therefore, it has attracted the interest of physicists and engineers from many application fields all over the world. In the last decade, significant efforts have been made to understand this heterogeneous structure, including formation of the clusters and the core-annulus structure. Useful information on cluster shape, size, internal structure and core region size etc. has been collected (Li & Kwauk, 1980; Horio & Kuroki, 1994; Sharma et al., 2000; Lackermeier et al., 2001). Also, it has been found that the system instability is closely related to the properties of the fluid-particle system. Systems with large fluid-solid density difference tend to form clusters more easily (Grace & Tuot, 1979). Particularly, the detailed analysis for particle-particle and particle-fluid interactions (normally based on a multi-scale method, e.g., Li & Kwauk, 2003) begins to shed light on finally unveiling the mechanism underlying heterogeneous flow structure formation in dense gas-solid flows.

However, owing to the complex and transient properties of dense gas-solid flows, the mechanisms underlying the origin and evolution of the heterogeneous flow pattern have not been completely elucidated. Some researchers suppose that the core-annulus structure results from the wall effect, which slows down the gas phase and forms a swarm of particle clusters. However, there are indications (Hoomans et al., 2000) that non-ideal particle-particle collisions cause formation of particle agglomerates and consequently lead to formation of a core-annulus flow structure. Furthermore, by employing discrete element simulation, Helland et al. (2000) demonstrated that non-linear drag also led to a heterogeneous flow structure.

In this paper, a computational study has been carried out to explore the mechanisms which control the cluster-dilute pattern formation by employing a discrete particle method (a "hard-sphere model" based on molecular dynamics). Particular attention is paid to both effects of gas-solid interaction and inelastic collisions between particles on pattern formation in high velocity gas-solid two-phase flows by employing a simple but powerful tool, namely energy budget analysis, to understand how the flow structures are related to these two phenomena. First, simulations will be performed using different particle collisional properties to quantitatively understand collisional dissipation induced instability. Then, simulations with different gas phase properties (drag force), but zero collisional dissipation will be carried out to explore the effect of gas-particle interaction on flow pattern formation. In addition, a system with strong collisional dissipation and enhanced gas-solid interaction (elevated pressure system) will be studied to highlight whether there exists a necessary condition between those two instability-inducing factors by which the heterogeneous flow structure is initialized. Finally, the evolution of flow structure with flow rate to the dilute transportation regime will be examined.

2. Theoretical Background

In our discrete particle model the gas phase is described by the volume-averaged Navier-Stokes equation, whereas the particles are described by the Newtonian equations of motion while taking particle-particle and particle-wall collisions into account. The original computer codes for solving these sets of equations were developed by Kuipers et al. (1992) for the gas phase and Hoomans et al. (1999) for the granular dynamics including both 2D and 3D geometries. Additional codes will be developed in this study to enable energy budget analysis.

2.1 Gas phase model

Continuity equation of a gas phase can be written as:

$$\frac{\partial(\varepsilon\rho_g)}{\partial t}+(\nabla\cdot\varepsilon\rho_g\boldsymbol{u})=0\,. \tag{1}$$

And corresponding momentum equation of the gas phase is expressed as follows:

$$\frac{\partial(\varepsilon\rho_g\boldsymbol{u})}{\partial t}+(\nabla\cdot\varepsilon\rho_g\boldsymbol{uu})=-\varepsilon\nabla p-\boldsymbol{S}_p-(\nabla\cdot\varepsilon\bar{\tau}_g)+\varepsilon\rho_g\boldsymbol{g}\,, \tag{2}$$

where the source term $\boldsymbol{S}_p$ ($N\cdot m^{-3}$) represents the reaction force to the drag force exerted on a particle per unit of volume suspension which is fed back to gas phase. In this work, transient, two-dimensional and isothermal flow of air at atmospheric and elevated pressure conditions is considered.

2.2 Granular dynamics model

Force balance for a single particle can be written as:

$$m_p\frac{d\boldsymbol{V}}{dt}=m_p\boldsymbol{g}+\frac{V_p\beta}{1-\varepsilon}(\boldsymbol{u}-\boldsymbol{V})-V_p\nabla p\,. \tag{3}$$

In Eq. (3), the third term on the right hand side represents the force due to the pressure gradient. The second term is due to the drag force, where β represents the interphase momentum exchange coefficient similar to that encountered in two-fluid models. The following well-known expression (Wen & Yu, 1966) has been used with n=2.7. Other values of n will also be used to examine the particle group effect in the simulation.

$$\beta=\tfrac{3}{4}C_d\frac{\varepsilon(1-\varepsilon)}{d_p}\rho_g|\boldsymbol{u}-\boldsymbol{V}|\varepsilon^{-n}\,. \tag{4}$$

The drag coefficient C_d is a function of the particle Reynolds number Re_p and is given by:

$$C_d=\begin{cases}\dfrac{24}{Re_p}(1+0.15Re_p^{0.687}) & Re_p<1000\\[2ex] 0.44 & Re_p\geq1000\end{cases}, \tag{5}$$

where Re_p is defined as:

$$Re_p=\frac{\varepsilon\rho_g|\boldsymbol{u}-\boldsymbol{V}|d_p}{\mu_g}\,. \tag{6}$$

2.3 Simulation technology

The hard sphere model is used to describe a binary, instantaneous, inelastic collision with friction between two particles. At any instant during the impact, the motions of the particles are governed by the linear and angular impulse-momentum laws. The key parameters of the model are the coefficient of restitution ($0<e<1$) and the coefficient of friction ($\mu>0$). The collisional dynamics and its computational implementation have been detailed by Hooomans et al. (1996). Here, we just introduce this method briefly. In this approach a sequence of binary collisions is processed. This implies that a collision list is compiled in which for each particle there is a collision partner and a corresponding collision time is stored. A constant time step is used to take the external forces into account and within this time step the prevailing collisions are processed sequentially. In order to reduce the required CPU time, neighbour lists and cell lists are used. For each particle a list of neighboring particles is stored and only for the particles contained in this list a check for possible collision partners is performed. The simulations are carried out only for the central part of the riser section without considering inlet and exit effects. A certain amount of particles is fed at the bottom at a specified velocity according to a prescribed solid mass flux. When particles approach the top they are removed from the system. The simulation conditions are listed in Table 1. Effects due to particle size distribution are not included in this research, but can be found in the literature (Hoomans et al., 2000; Hoomans et al., 2001).

Table 1 Simulation conditions for base case: run 1

System	Bed height / m	2
	Width / m	0.08
Particles	Density / $kg\cdot m^{-3}$	2600
	Diameter / μm	500
	Solids flux / $kg\cdot m^{-2}\cdot s^{-1}$	25
	Inlet velocity / $m\cdot s^{-1}$	0.4
	Restitution coef. e	0.95
	Friction coef. μ	0.30
Gas velocity / $m\cdot s^{-1}$		5 (23 u_{mf})
Pressure / MPa		0.12
Simulation grid		20×100
Voidage exponent n		4.7
dt / ms		0.1

Conditions for run 2: same as run 1 except: e =1.0, μ =0; (run 2b: G_s=75 $kg\cdot m^{-2}\cdot s^{-1}$).
run 3: same as run 2 except: voidage exponent n=0.
run 4: same as run 1 except: pressure 5 MPa, U_g=1.68 $m\cdot s^{-1}$ (23 u_{mf}, 5 MPa).
Refer to legends for other conditions

2.4 Energy analysis

In fluid-particle systems, there exist two types of interactions: fluid-particle interaction due to drag and particle-particle interaction due to collisions. Our hard sphere based DPM model accounts for these two interactions in great detail. Different from the soft-sphere based DEM model in which the so-called “time-driven” strategy (i.e., specifying a time step in advance) is usually employed to

locate the collisional partners, the DPM model uses the "event-driven" technique for the collisional pair search, allowing for a variable simulation time step automatically determined by the collisional sequence (event). As a result, this not only saves a lot of CPU time when the system is in its dilute state, but also prevents the possible simulation error of missing certain amount of collisions when a large time step is improperly selected. Therefore, DPM guarantees the correct collisional dynamics. In addition, for every individual particle collision, the various properties can be precisely calculated with respect to its force, motion and energy dissipations including both compression and frictional energies. Consequently, the hard sphere model enables quantitatively computing the various work terms and energy types for the entire system during the process. On such a basis, we are capable of exploring the underlying mechanisms which control flow pattern formation. The various energy calculations have been described in detail in our earlier paper (Li & Kuipers, 2002). Here we only present the energy budget analysis for circulating fluidized beds.

The particle phase energy analysis includes: 1) energy input (work) to the particulate phase, which is composed of the work done by the drag force W_{drg}, initial energy of the system E_{tot}, and energy introduced by newly fed particles $E_{\mathrm{inp,tot}}$; 2) energy budget distribution in the particulate phase, including kinetic E_{kin}, rotational E_{rot}, potential energies E_{pot} and collisional dissipation E_{dsp}. For circulating fluidized beds, the energy carried by outgoing particles should also be taken into account. According to the energy conservation principle for the particulate phase, the relationship between work done by drag and these energies is expressed as follows:

$$W_{\mathrm{drg}} = E_{\mathrm{dsp}} + \Delta E_{\mathrm{pot}} + \Delta E_{\mathrm{kin}} + \Delta E_{\mathrm{rot}} \,. \tag{7}$$

For a circulating fluidized bed, we have:

$$W_{\mathrm{drg}} = E_{\mathrm{dsp}} + (E_{\mathrm{pot}} + E_{\mathrm{pot,out}}) + (E_{\mathrm{kin}} + E_{\mathrm{kin,out}}) + (E_{\mathrm{rot}} + E_{\mathrm{rot,out}}) - E_{\mathrm{inp,tot}} - E^{0}_{\mathrm{tot}}. \tag{8}$$

In addition to the absolute energy, a parameter of the energy partition fraction is defined to characterize the fractional energy budget:

$$f_i = \frac{E_i}{W_{\mathrm{drg}} + E^{0}_{\mathrm{tot}} + E_{\mathrm{inp,tot}}} \,, \tag{9}$$

where the subscript i refers to either of total particle collisional dissipation, kinetic, rotational and potential energies respectively.

3. Results and Discussions

3.1 Collisional dissipation induced instability

Fig. 1(a) shows the snapshot of the flow patterns for e=0.95, μ=0.30. Compared to the flow pattern under conditions of ideal collisions (see Fig. 1(b)), the case with non-ideal collisions produces a flow structure containing (dense) clusters. Also, the particle hold-up in the non-ideal

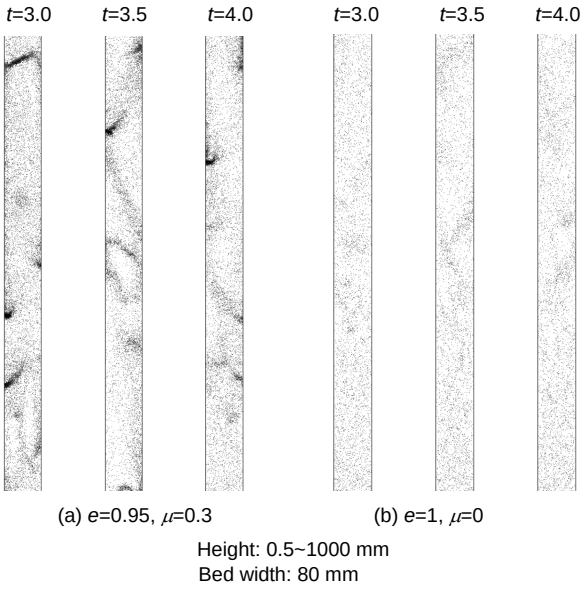

Fig. 1 Flow structures in a CFB: effect of collisional dissipation.

case is higher than that with ideal collisions. The energy budget analysis presented in Fig. 2 clearly demonstrates that a higher fractional component of energy is consumed due to collisional dissipation, which greatly reduces both the particle potential and kinetic energy. This conclusion is similar to that drawn from a previous study on bubbling fluidized beds (Li & Kuipers, 2001). Once non-ideal particle-particle collisions prevail, a certain amount of energy is consumed due to the collisional dissipation. Particles obtain less energy to suspend themselves freely in space (raising potential energy). When new particles are encountered, additional dissipation occurs and the process repeats itself. If fluid-solid interaction is not strong enough to prevent the particles to approach each other, eventually a "particle cluster" is formed.

However, unlike the situation in dense gas-fluidized beds where particle clusters form as a continuous phase, all initial particle clusters in circulating fluidized beds can not connect each other to form a continuous emulsion phase, but only exist as individually separated "particle islands". This stems from the much stronger gas-solid interaction in a CFB (potential energy fraction up to 80%, in Fig. 2) compared to that in dense bubbling beds (only 20%, Li & Kuipers, 2001). In other words, although collisional dissipation results in flow instability in both cases, owing to the fundamental change of particle-particle controlled interaction giving way to gas-solid controlled interaction, only local heterogeneity is displayed in a circulating fluidized bed. For this mode of cluster formation mechanism, two conditions are necessary: one is that the collision actually has to occur and the other is that the collisions should be accompanied by energy dissipation. Should one of them not be fulfilled, a dissipation induced heterogeneous structure would be impossible. However, it should be noted in Fig. 1(b) that some degree of flow heterogeneity still exists. The

question arises immediately: what causes this heterogeneity then? In the next section, we will address this problem by analyzing the ideal collisional system — the most fundamental mechanism directly underlying the instability in high-velocity gas fluidized beds.

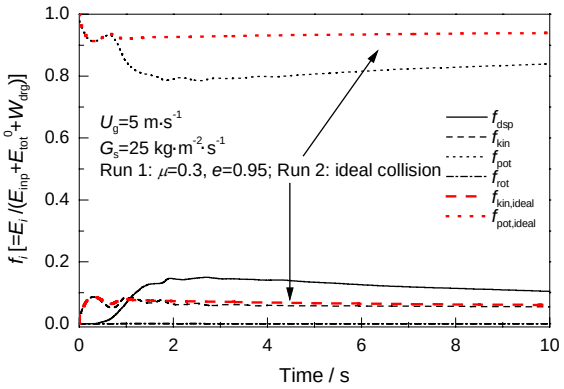

Fig. 2 Energy analysis in a circulating fluidized bed: effect of collisional dissipation, where the vertical axis f_i denotes the ratio of each type of particle energy to the total energies in the system and the horizontal axis is the simulation time. There are no collisional and rotational energy dissipations for the ideal case.

3.2 Non-linear gas drag induced instability

Many researchers have found from experiments that fluidization quality is closely related to the voidage exponent (2.35~4.7) in the well-known Richardson-Zaki (referred to as "R-Z" subsequently) equation, small values correspond to good fluidization quality or a uniform flow pattern. Unfortunately, a theoretical formulation to fully predict the drag force for such a dynamic system is still not available. Based on the R-Z correlation, Wen & Yu (1966) derived a drag correlation for a group of particles immersed in a fluid (most of them are liquids). In this well-known correlation a voidage exponent of 4.7 is employed. However, this fixed value is only valid in the high (>500) and low (>2) Reynolds number regime (see Felice, 1994).

Particularly, there exists some experimental evidence indicating that for most gas-solid systems, the voidage exponent n in R-Z equation is actually more disperse, far deviating from 4.7 for some cases, especially for very small cohesive powders and for large and heavy particles (e.g., see Mogan et al., 1970/1971; Makkawi & Wright, 2003). From Mogan's detailed statistics of the voidage exponent of n in R-Z equation for a series of gas-solid systems, one would realize the necessity to reconsider this problem. He showed that the averaged n value for a group of particles in gas centers around 0.94, much smaller than the conventional value of 4.7. However, this center shifts up to 6.0 for systems with very large particles. It suggests that with increasing value of n, or the non-linearity of the system, a more heterogeneous gas-solid system develops for low-velocity gas-fluidized beds. This has been confirmed by the authors' numerical research (Li & Kuipers, 2003).

In retrospect of the historic background for developing R-Z correlation and Wen-Yu equation (Wen & Yu, 1966), we came to be aware that these semi-empirical and empirical equations were all established on the force balance assumption (equilibrium) for each suspended particle. Without any doubt, such a condition is suited to most liquid-solid systems. Unfortunately, it did not always hold for most gas-solid flows — a system far away from equilibrium (see Li & Kuipers, 2003). It is accordingly necessary to carefully examine such a system in order to understand how this non-linearity affects the instability in high-velocity gas fluidization to see if we can trace its fundamentals.

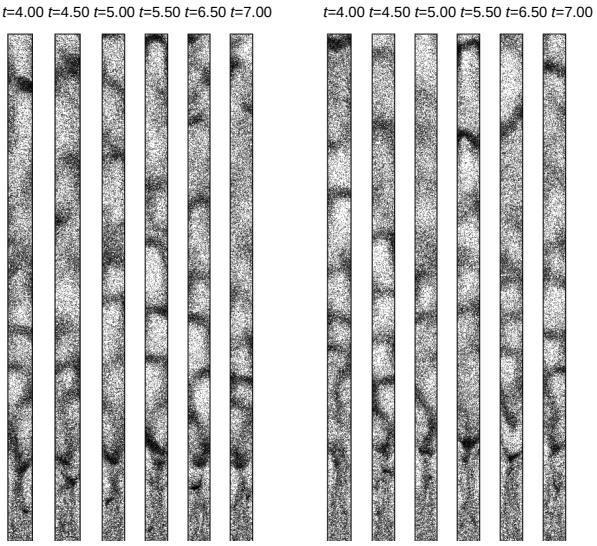

Fig. 3 Flow structures in a CFB: effect of non-linear drag (ideal collisions, C_d=$C_{d,single}\varepsilon^{-n}$). Solid flux is 75 kg·m^{-2}·s^{-1}. The other conditions are the same as those in Table 1.

Fig. 3 shows snapshots taken from the simulations with ideal collisions using the voidage exponents of 0 and 4.7 in the drag formulation respectively. Note that a value of n equal to 0 implies no effect of neighbour particles on the drag. Since this particle group effect on drag force is insensitive at low solid fraction, a higher solids flux of 75 kg·m^{-2}·s^{-1} has been employed in these simulations. In addition, the domain-averaged mean square solid volume fraction fluctuation, defined below, is used to quantitatively characterize and compare the flow structures:

$$< f_s'^2 >= \frac{1}{NR \cdot NZ} \sum_{i=1}^{NR} \sum_{j=1}^{NZ} (f_{s,i,j} - \bar{f}_s)^2 , \qquad (10)$$

where NR and NZ are the numbers of computational cells in respectively the radial and axial direction, and $f_{s,i,j}$ is the solids volume fraction in cell (i, j). The bar represents the domain-averaged value. The results are shown in Fig. 4. Clearly, particle clusters still exist in the system with ideal particle collisions. Our results indicate that a large voidage exponent produces a more uniform flow structure in high-velocity gas-fluidized beds.

A comparison of the energy budget analysis for n=0 and n=4.7 focusing on the kinetic and potential energies (no dissipation and rotation due to ideal collision) is shown in Fig. 5 indicating that the dominant drag force distributes a greater portion of the energy to particle kinetic energy.

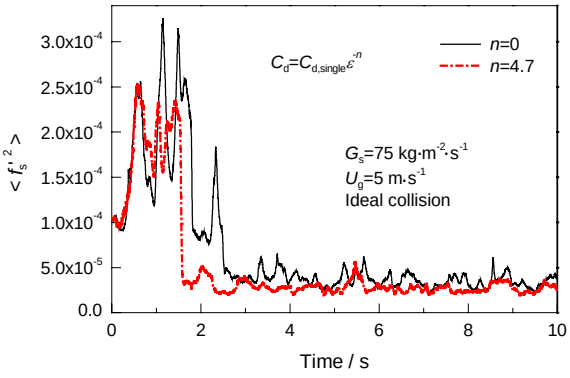

Fig. 4 Domain-averaged mean square solids volume fraction fluctuation: effect of exponent n in drag equation.

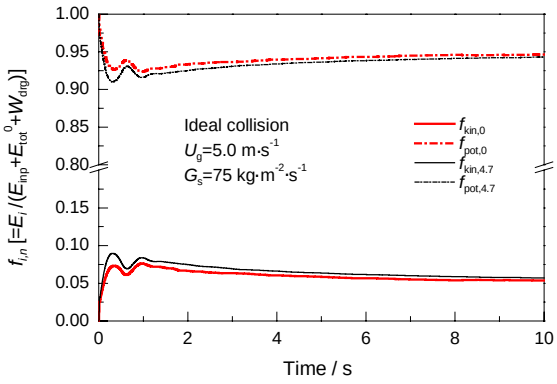

Fig. 5 Energy analysis in circulating fluidized beds: effect of non-linear drag.

In addition, the domain-averaged granular temperature, defined in Eq. 11, is shown in Fig. 6 indicating that a bigger voidage exponent results in fewer collisions of particles. This means that a stronger group effect reduces the particle fluctuation motion and therefore the collision tendency. As a result, it results in a more homogeneous flow structure in circulating fluidized beds.

$$< T >= \frac{1}{NR \cdot NZ \cdot \bar{f}_s} \sum_{i=1}^{NR} \sum_{j=1}^{NZ} (f_{s,i,j} T_{i,j}) \,, \qquad (11)$$

where

$$T_{i,j} = \frac{1}{2} \frac{\sum_{k=1}^{N_{i,j}} (c_{k,x} - \bar{c}_x)^2 + \sum_{k=1}^{N_{i,j}} (c_{k,y} - \bar{c}_y)^2}{N_{i,j}} \,. \qquad (12)$$

From Fig. 5, it is noticed that the greater portion of energy distributed to kinetic motion leads to a relatively more homogeneous flow structure (n=4.7), which is different from the case for bubbling beds. Compared to the convection energy distributions in Fig. 6, we notice that this increased portion is distributed to translational particle motion (for shifting), but not for convection (for colliding), both being the necessary components of kinetic energy. In high-velocity gas fluidization, it not only requires enough potential energy to keep the particle in suspension, as the case for bubbling beds (see Li & Kuipers, 2002), but also to provide significant amount of translational energy for particle transportation. Obviously, the latter part is not necessary for bubbling beds. Also, translational motion does not induce any flow instability.

Therefore, it is very important to distinguish the convection portion of energy and collisional dissipation from the total particle energy drawn from the gas phase when one attempts to understand pattern formation in gas-solid two-phase flows.

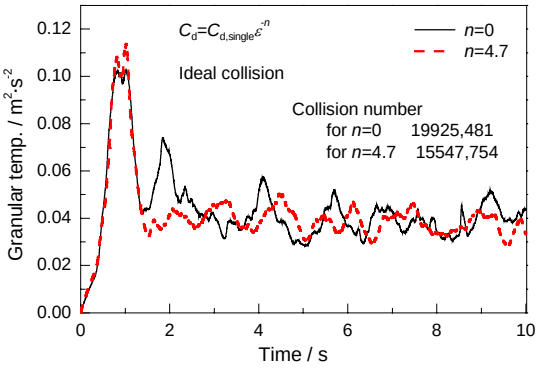

Fig. 6 Granular temperature in CFB: effect of non-linearity of drag or group effect.

3.3 Combined effect of particle collision and gas drag

As shown above, both non-ideal particle-particle collision and non-linear drag could produce heterogeneous flow structures. However, the respective conditions and their induced cluster structures are different and therefore also a case was studied in which the combined effect of non-ideal particle-particle collision and strong gas-solid interaction was considered.

Fig. 7 shows the simulation results of run 4 with non-ideal particles at an elevated pressure of 5 MPa and superficial gas velocity of 1.68 m·s^{-1} (23u_{mf}), — a strongly "fluid-controlled" system. Interestingly, we obtain a homogeneous flow structure. This demonstrates that collisional dissipation can only play a role in case collisions can actually occur. In other words, it is not the necessary condition for heterogeneous flow structure formation. This could also be employed to explain the homogeneous flow patterns observed in most of the liquid-solid systems. Corresponding energy analysis, as shown in Fig. 8, indicates that nearly all energy is employed to suspend particles in such a case, implying that particles are always in an equilibrium state.

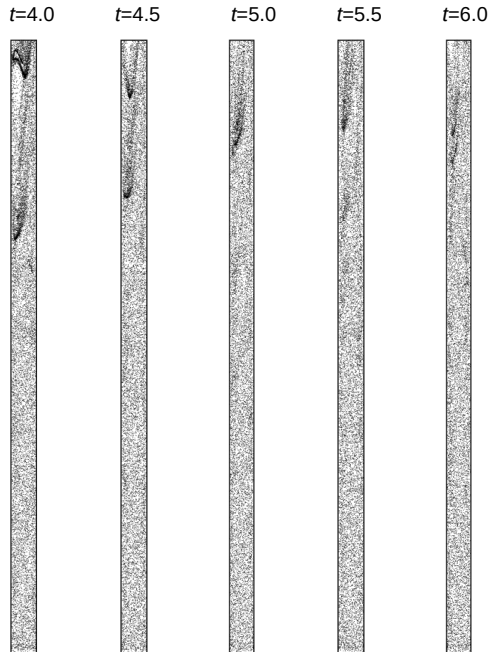

Fig. 7 Flow structure in a CFB at elevated pressure (run 4): homogeneous flow structure.

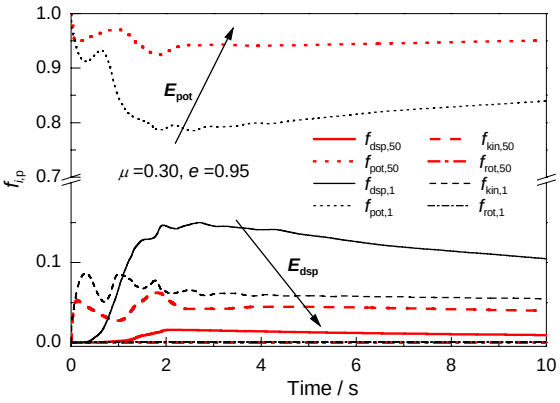

Fig. 8 Comparison of energy budget analysis for the dissipation suppressed system at elevated pressure and the normal system at atmosphere pressure.

Different from cluster formation driven by collisional dissipation, the non-linear drag-induced cluster formation mechanism, which depends on the flow regime and material properties (density and particle size), always plays a role if the drag force in the system has the non-linear voidage-dependent property. For circulating gas-fluidized beds operating at atmospheric conditions, owing to the large density difference, the non-linearity of the drag force always exists or particles are always in a non-equilibrium motion. Therefore, it is the fundamental source leading to particle agglomerates. Non-linear drag force has a “phase separation” function, which definitely enhances particle-particle collision. If the drag-force-induced particle collisions are non-ideal, it further intensifies particle agglomeration.

3.4 Particle motion in circulating gas-fluidized beds

Compared to the influence of non-linear drag on flow structure in bubbling fluidized beds, the influence of non-linear drag on flow structure in circulating fluidized beds shows an opposite trend, that is, in bubbling flow, the system with stronger voidage dependence tends to form a more heterogeneous flow structure but a more homogeneous flow structure in circulating fluidized beds.

In order to obtain an insight into local cluster formation in circulating fluidized beds, it is necessary to understand the particle dynamics, both inside and outside of a cluster. Single particle motion and its aggregating status, in term of its neighboring particle number, will be monitored focusing on its position, velocity and acceleration in a circulating fluidized bed with both ideal collision and non-ideal collision. When the particle being monitored leaves the system, a new fresh particle is monitored again. The analysis is specific to particles located in the central region in a riser (run 2b).

From circulating fluidized bed simulations, two typical particle “group” effects can be identified. The first “group” effect is to greatly suppress the otherwise accelerating motion of the particles. This effect prevails in the bottom and in the annular regions of the circulating fluidized bed, that is, collectively, in the dense particle regions. Figs. 9 and 10 show these cases respectively. The flow typically displays the presence of clusters undergoing obvious deceleration (i.e., smaller drag acting on each particle inside) and individual particles experiencing considerable acceleration (i.e., larger drag). This phenomenon is opposite to the cases in bubbling gas-fluidized beds where the individual particle in the dilute region is decelerated, but accelerated while it stays in the dense region (Li & Kuipers, 2003).

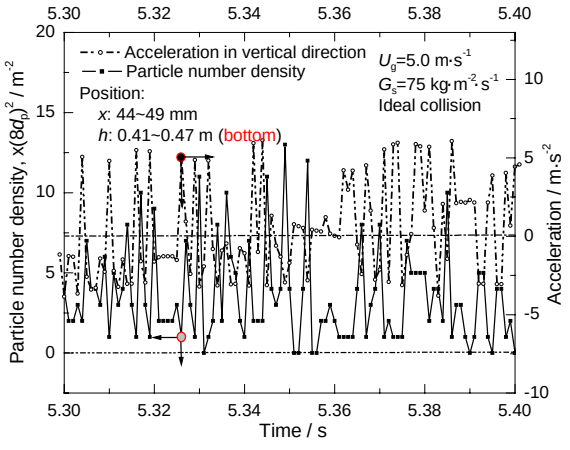

Fig. 9 Influence of particle group effect on particle motion in a circulating fluidized bed at the bottom region (run 2b): suppressing the otherwise accelerated individual particles, where x and h represent respectively the radial and axial positions.

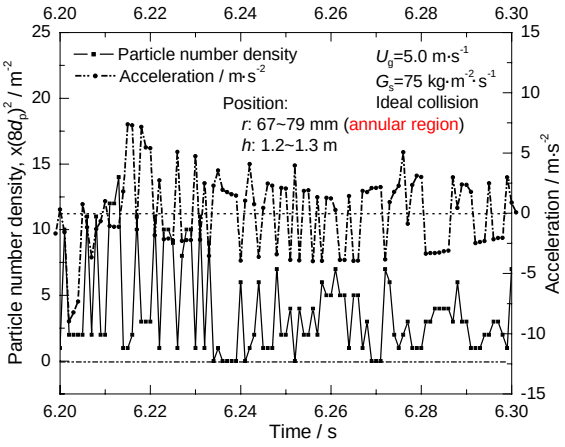

Fig. 10 Influence of particle group effect on particle motion in a circulating fluidized bed in the annular region (suppressing the otherwise accelerated individual particles, where *x* and *h* represent respectively the radial and axial positions).

This difference lies in the fact that in a high-velocity gas-fluidized bed the local gas velocity is most likely greater than the terminal velocity of a single particle. Consequently, individual particles can be easily lifted even without the enhancement induced by this "group" effect. However, this is not the case for the bubbling gas-fluidized beds. Also, being a component of the dispersed phase, the particles in a cluster experiences a reduced drag force since not all the gas is necessarily required to penetrate the dense cluster in order to pass through and then escape the bed from the continuous dilute path. Therefore, the clusters formed tend to fall down. This has been demonstrated experimentally in the dense regions, e.g., near the wall, in a circulating fluidized bed (Horio & Kuroki, 1994).

The second "group" effect is to maintain a high particle shifting velocity, otherwise the individual particle tends to decelerate, as demonstrated in Fig. 11. This phenomenon is observed in the middle section and near the bed center though the particle tends to maintain its stable state (force balance, i.e., zero acceleration). When the particle runs outside of a cluster, it decelerates. However, because of weak clustering in the central region, its impact on flow structure formation would be limited.

Similar results are found in circulating fluidized beds with non-ideal collisional particles (see Fig. 12).

The fundamental difference between these effects originates from the difference of flow state of the cluster: a cluster moves slowly in the dense region but fast in the fully developed region. Therefore, the particle "group" effect leads to two opposite results depending on the local hydrodynamics. Since the extent of clustering is naturally determined by system properties, reflected by the voidage function, the systems with a strong group effect (large voidage function exponent) can effectively, or even exponentially, increase the drag force acting on the particles inside the clusters to reduce the difference in forces acting on particles inside and outside of a cluster such that it suppresses the heterogeneous flow structure in dense regions. Unfortunately, at the same time it enlarges the difference in the dilute region, deteriorating its homogeneity to result in a more pronounced heterogeneous local flow structure. Considering weak clustering in the central region as compared to that in the dense region, we therefore expect to have a collectively improved gas-solid contact in high-velocity gas-fluidized beds in the case of systems having a strongly non-linear dependence of gas drag upon voidage. This has been proved in the last section. In the other words, the non-linearity of drag possesses a "phase melting" function in the high-velocity gas-fluidized beds in effectively lifting the particles inside the clusters to promote the formation of a homogeneous flow structure.

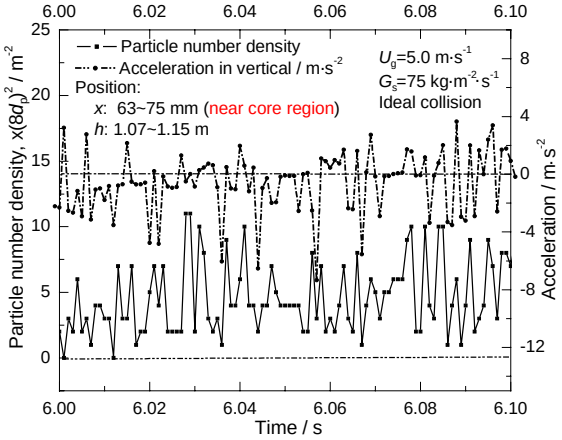

Fig. 11 Influence of particle group effect on particle motion in a circulating fluidized bed near the core region (promoting the otherwise decelerated individual particles, where *x* and *h* represent respectively the radial and axial positions).

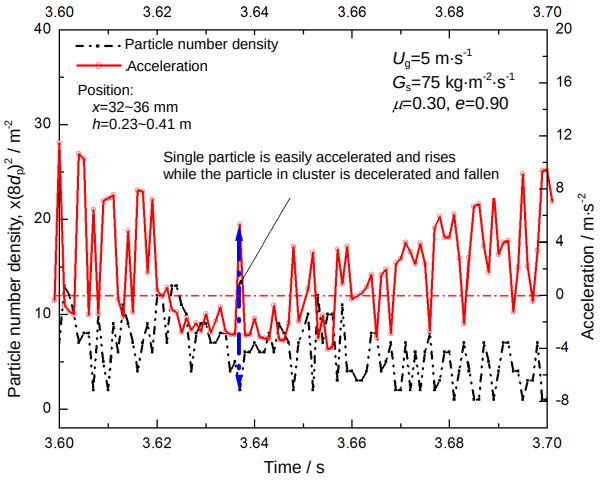

Fig. 12 Comparison of particle motions inside and outside of a cluster in a circulating gas-fluidized bed with non-ideal collisional particle at the bottom region (group effect suppresses the accelerated individual particle motion, voidage exponent equals 4.7 where *x* and *h* represent respectively the radial and axial positions).

3.5 Regime transition to dilute flow

Regime transition to dilute transportation has also been simulated to reveal flow structure evolution. In the simulation, the circulating rate of solids is fixed while the gas velocity is increased to observe the regime transition. Since the bed experiences an unstable process in the initial period of simulation (which should be excluded during the time-averaging calculation to obtain the flow structure profiles), time-averaged solids mass flux is monitored against the input solids flux.

Fig. 13 (inset) presents the time-averaged solids flux as a function of time. Clearly, after a certain period of operation, the system gradually becomes stable: the output flux equals the input flux. For high gas velocity, this period is quite short (1 s in the case of 9 $m \cdot s^{-1}$, or 3 s in the case of 5 $m \cdot s^{-1}$). To compare the flow structures on the same basis, the initial 3 seconds for all runs will be excluded accordingly. Interestingly, it is also observed that the fluctuation of the time-averaged mass flux of output solids is significantly reduced with increasing gas velocity as shown in Fig. 13. This demonstrates that the system transfers from a heterogeneous flow structure to a homogeneous one.

The variation of flow structures with gas velocity in terms of the time-averaged radial and axial solids volume fractions are presented in Figs. 14 and 15 respectively. Fig. 16 shows snapshots of the flow structures.

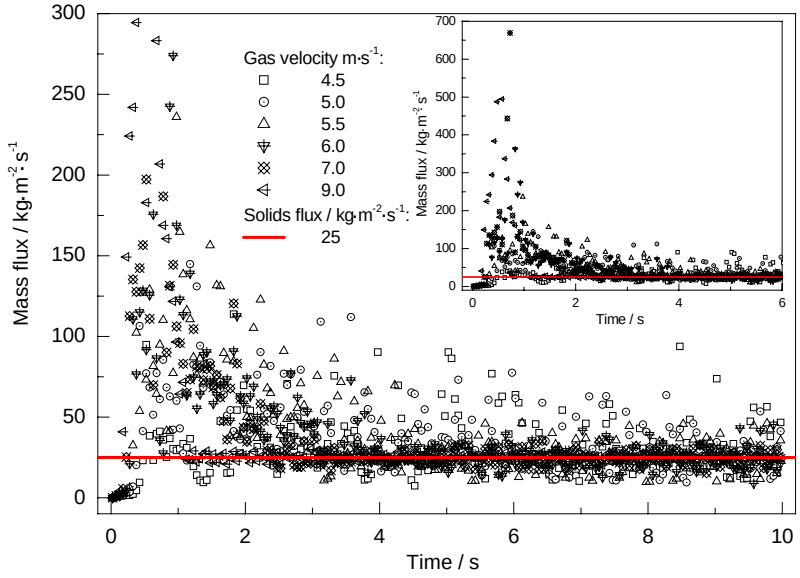

Fig. 13 Variation of the time-averaged mass flux of output particles with time: effect of superficial gas velocity: increasing gas velocity damps the fluctuation of solids circulating flux (inset: all systems become stable approximately after 3 seconds).

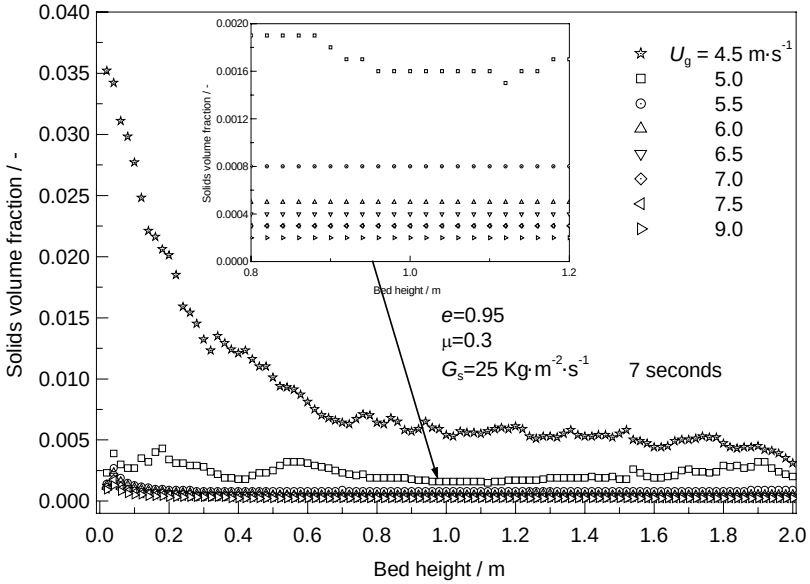

Fig. 14 Evolution of flow structure with gas velocity in a circulating fluidized bed: regime transition to dilute transportation (time-averaged solids volume fraction versus height is plotted, and flow structures at both micro- and macro-scales tend to homogeneity).

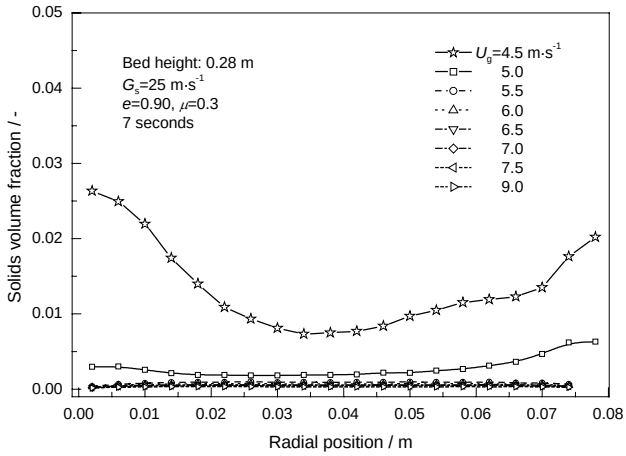

Fig. 15a Evolution of flow structure with gas velocity in a circulating fluidized bed and transition to dilute transportation: the time-averaged radial solids volume fraction distribution at the bottom.

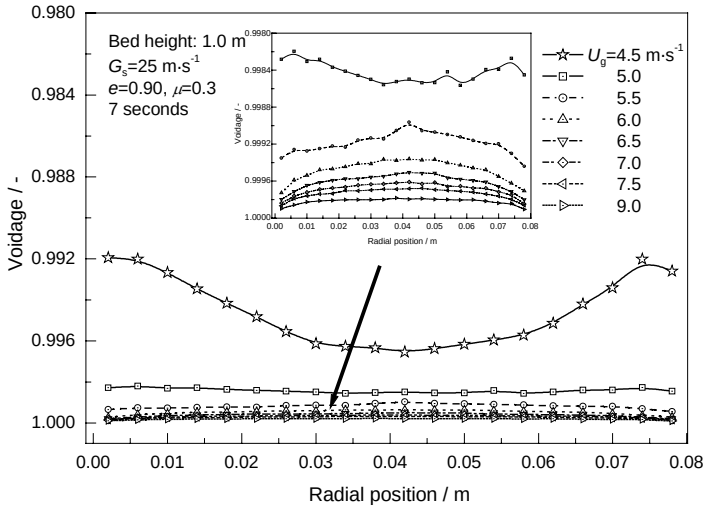

Fig. 15b Evolution of flow structure with gas velocity in a circulating fluidized bed and transition to dilute transportation: the time-averaged radial solids volume fraction distribution in the middle.

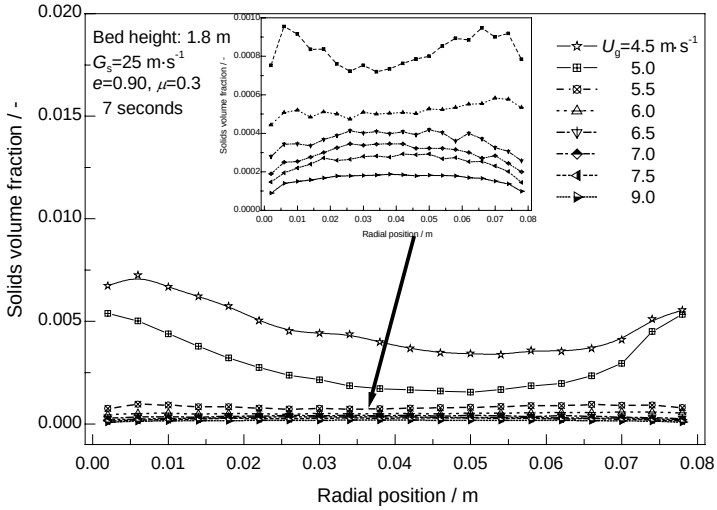

Fig. 15c Evolution of flow structure with gas velocity in a circulating fluidized bed and transition to dilute transportation: the time-averaged radial solids volume fraction distribution on the top.

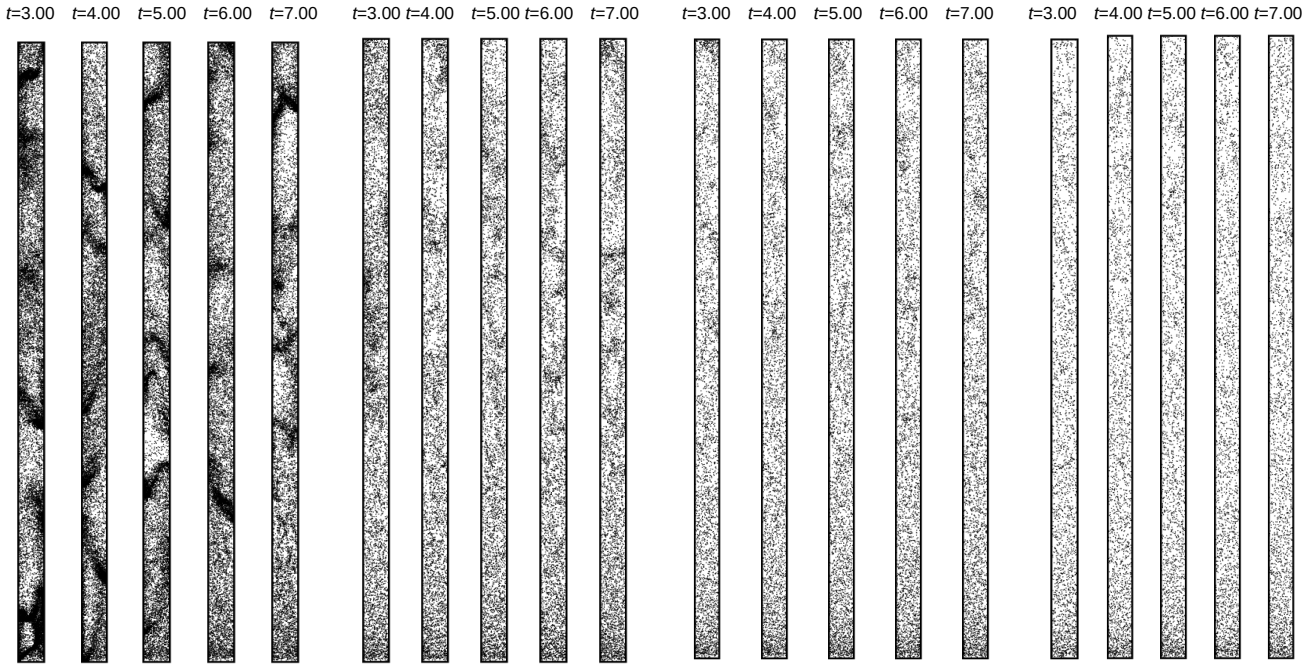

(a) U_g=5.0 m·s^{-1} (b) U_g=6.0 m·s^{-1} (c) U_g=7.0 m·s^{-1} (d) U_g=9.0 m·s^{-1}

Fig. 16 Evolution of flow structure with gas velocity in a circulating fluidized bed and transition to dilute transportation: snapshots of the flow structure. The systems become uniform and produce a uniform flow regime. Operation conditions are: non-ideal collisional particles with e=0.95 and μ=0.3.

As expected, with increasing gas velocity the flow structure becomes more homogeneous at both micro-scale and macro-scale. When the gas velocity exceeds a critical value (5.5 m·s^{-1} in this case), the system suddenly enters the dilute transportation mode, the dense bottom zone disappears and, instead, a homogeneous flow structure prevails in the system. In both radial and axial directions a relatively flat time-averaged distribution of solid volume fraction is obtained. Although the solids volume fraction profiles are flat, small spatial variations can still be recognized. When the gas velocity exceeds 5.0 m·s^{-1}, the solids volume fraction across the bed exhibits a profile which is opposite to the normal profile corresponding to the "core-annulus" structure, with low solid concentration near the wall (similar to the fluid velocity distribution). This suggests that the gas phase completely controls the particle motion (shifting) and consequently a second uniform flow regime (against the uniform regime after initial fluidization) is obtained.

Gas-solid systems are naturally open and dissipative — far from equilibrium. From the above-mentioned evidences, we can readily understand that this instability is induced by weak gas suspension, non-linearity of gas-solid interaction (upon voidage) and particle collisional dissipation. Among them, effective gas suspension is the key issue for achieving a homogenous flow structure and, to a great extent, approach to system equilibrium. From R-Z equation, we have learned that it is the fluid suspension capacity (Re_t) that physically determines the nonlinearity of fluid-solid interaction. The non-linear drag, in turn, controls particle convection, directly exercising its impact on particle collisional dissipation. Therefore, it can be concluded that the instability in gas-fluidized beds originates from weak gas suspension (induced convection) and is aggravated thereby by induced dissipative inter-particle collisions.

Consequently, we can manipulate and design novel processes and equipment, approaching and eventually achieving the equilibrium system, by properly utilizing such understandings. Now, such idea seems not impossible. The examples to be listed show very promising signs along this direction: uniformly fluidized nano-gel powders in gas flow, uniform catalyst suspensions in supercritical fluids, improved fluidization quality by nano-coating (through reducing collisional energy dissipation), etc.

4. Conclusions

In summary, high-velocity gas-solid flows are dissipative, non-linear and far from equilibrium, normally tending towards heterogeneous flow structures. This research demonstrates that the competition between gas-particle interaction, including those for both particle suspension (associated with potential energy) and transportation (associated with translational energy), and particle-particle interaction, including both convective motion (associated with particle random motion or granular temperature) and particle collisional dissipation (associated with dissipative energy) — fully determines the formation of various flow structures. When gas-solid interaction dominates, a sys-

tem decisively displays a homogeneous flow structure, as evidenced by the cases involving elevated system pressure, higher velocity (>5.5 $m \cdot s^{-1}$) such as for circulating fluidized beds. Different from the case for bubbling beds, particle transportation (besides suspension) also plays an even more important role of homogenization such as in high-velocity gas-fluidized beds.

However, when gas-solid interaction becomes weak, flow instability occurs. The system displays heterogeneous flow structures, including both local particle clusters and other uneven spatial voidage distributions on the macro-scale.

Two kinds of mechanisms, that is, the non-linear dependence of gas drag force upon voidage and particle collisional dissipation, have been identified, which underlie the above-mentioned instability and lead to the formation of heterogeneous flow structure.

Simulation of a CFB system has showed that a smaller "group" effect in the drag correlation produces a more pronounced heterogeneous flow pattern since the particle "group" effect is so sensitive as to provide a strong enough force to lift the particles inside the clusters. The difference of drag forces acting inside and outside of a transient cluster is, therefore, enlarged, leading to more intensive particle convection. Consequently, inter-particle dissipative collision begins to play its role. And a significant amount of energy, drawn from the gas phase, is therefore consumed. As a result, a uniform suspension system collapses. Of these two mechanisms, the non-linear drag force or gas-solid interaction is obviously the key to initializing the heterogeneous flow structure. Particle "group" effect plays an opposite function in circulating fluidized beds by activating the otherwise decelerated individual particles in dilute regions. Further work is however required to confirm this point.

Flow regime transition can also be highlighted accordingly. As gas flow velocity increases to exceed a certain critical value, the flow suddenly transforms to the uniform dilute transportation regime. To achieve a fully homogeneous flow structure controlled by gas suspension all over the bed, it is necessary, however, to operate at even higher gas velocities.

Nomenclature

C_d	drag coefficient
d_p	particle diameter, m
e	coefficient of restitution
E	energy, J
$\boldsymbol{F}$	force, N
G_s	solids circulating rate, $kg \cdot m^{-2} \cdot s^{-1}$
f_s	solids volume fraction
f	energy fraction
$\boldsymbol{g}$	gravitational acceleration, $m \cdot s^{-2}$
h, r	horizontal position, m
m_p	particle mass, kg
NR	grid number in horizontal direction
NZ	grid number in vertical direction
p	pressure, Pa
Re_p	particle Reynolds number
$\boldsymbol{S}_p$	source term defined in Eq. 2
t	time, s
$\boldsymbol{u}$	gas phase velocity, $m \cdot s^{-1}$
U_g	superficial gas velocity, $m \cdot s^{-1}$
$\boldsymbol{V}$	velocity, $m \cdot s^{-1}$
V	volume, m^3
$\boldsymbol{W}$	work, J
x	radial position, m

Greek letters

β	Volumetric inter-phase momentum transfer coefficient, $kg \cdot m^{-3} \cdot s^{-1}$
ε	void fraction
μ_g	gas shear viscosity, $kg \cdot m^{-1} \cdot s^{-1}$
θ	granular temperature, K
ρ	density, $kg \cdot m^{-3}$
$\boldsymbol{\tau}$	gas phase stress tensor, $kg \cdot m^{-1} \cdot s^{-2}$

Subscripts

0	initial condition
buoy	buoyancy
drg	drag
dsp	dissipated
g	gas phase
inp	input
kin	kinetic
out	output
p	particle
pot	potential
rot	rotational
s	solid
tot	total

References

Felice, R. D. (1994). The voidage function for fluid-particle interaction systems. *Int. J. Multiphase Flow*, 20, 153−159.

Grace, J. R. & Tuot, J. (1979). A theory for cluster formation in vertically conveyed suspensions of intermediate density. *Trans. Inst. Chem. Eng*., 57, 49−54.

Helland, E., Occelli, R. & Tadrist, L. (2000). Numerical study of cluster formation in a gas-particle circulating fluidized bed. *Powder Technol.*, 110, 210−221.

Hoomans, B. P. B., Kuipers, J. A. M., Briels, W. J. & van Swaaij, W. P. M. (1996). Discrete particle simulation of bubble and slug formation in a two-dimensional gas-fluidised bed: a hard-sphere approach. *Chem. Eng. Sci*., 51, 99.

Hoomans, B. P. B., Kuipers, J. A. M., Salleh, M. A. M., Stein, M. & Seville, J. P. K. (2001). Experimental validation of granular dynamics simulations of gas-fluidised beds with homogenous in-flow conditions using positron emission particle tracking. *Powder Technol.*, 116, 166−177.

Hoomans, B. P. B., Kuipers, J. A. M. & van Swaaij, W. P. M. (1999). Discrete particle simulation of cluster formation in dense riser flow. In Werther, J. (Ed.), *CFB-VI* (pp.255−260). Wurzburg.

Hoomans, B. P. B., Kuipers, J. A. M. & van Swaaij, W. P. M. (2000). Granular dynamics simulation of segregation phenomena in bubbling gas-fluidized beds. *Powder Technol.*, 109, 41−48.

Horio, M. & Kuroki, H. (1994). Three dimension flow visualization of dilutely dispersed solids in bubbling and circulating fluidized bed. *Chem. Eng. Sci*., 49, 2413−2421.

Kuipers, J. A. M., van Duin, K. J., van Beckum, F. P. H. & van Swaaij, W. P. M. (1992). A numerical model of gas-fluidized beds. *Chem. Eng. Sci*., 47, 1913−1924.

Lackermeier, U., Rudnick, C., Werther, J., Bredebusch, B. & Burkhardt, H. (2001). Visualization of flow structures inside a circulating fluidized bed by means of laser sheet and image processing. *Powder Technol.*, 114, 71−83.

Li, J. & Kuipers, J. A. M. (2001). Effect of pressure on flow behaviors in dense gas-fluidized beds: a discrete particle simulation study. In Kwauk, M., Li, J. & Yang, W.-C. (Eds.), *Fluidization X* (pp.389−396). Beijing: Engineering Foundation, Inc.

Li, J. & Kuipers, J. A. M. (2002). Effect of pressure on flow behaviors in dense gas-fluidized beds: a discrete particle simulation study, extended version. *Powder Technol.*, 127, 73−84.

Li, J. & Kuipers, J. A. M. (2003). On the origin of heterogeneous flow structures in dense gas-solid flows. *Chem. Eng. Sci.*, submitted.

Li, J. & Kwauk, M. (2003). Exploring complex systems in chemical engineering — the multi-scale methodology. *Chem. Eng. Sci*., 58, 521−535.

Li, Y. & Kwauk, M. (1980). The dynamics of fast fluidization. In Grace, J. R. & Matsen, J. M. (Eds.), *Fluidization-III* (pp.537−544). Plenum Press.

Makkawi, Y. T. & Wright, P. C. (2003). The voidage function and effective drag force for fluidized beds. *Chem. Eng. Sci.,* 58, 2035−2051.

Mongan, J. P., Taylor, R. W. & Booth, F. L. (1970/1971) The value of the exponent *n* in the Richardson and Zaki equation, for fine solids fluidized with gases under pressure. *Powder Technol.*, 4, 286−289.

Sharma, A. K., Tuzla, K., Matsen, J. & Chen, J. C. (2000). Parametric effects of particle size and gas velocity on cluster characteristics in fast fluidized beds. *Powder Technol.*, 111, 114−122.

Wen, C. Y. & Yu, Y. H. (1966). Mechanics of fluidization. *Chem. Eng. Prog. Symp. Ser*., 62, 100−111.

Manuscript received September 2, 2003 and accepted December 12, 2003.